

Measurement of the Cosmic Neutrino Flux from the Southern Sky using 10 years of IceCube Starting Track Events

The IceCube Collaboration

(a complete list of authors can be found at the end of the proceedings)

E-mail: msilva@icecube.wisc.edu, sarah.mancina@icecube.wisc.edu, josborn@icecube.wisc.edu

The measurement of a diffuse astrophysical neutrino flux using starting track events marks the first time IceCube has observed and subsequently measured the astrophysical diffuse flux using a dataset composed primarily of starting track events. Starting tracks combine an excellent angular and energy resolution. This enables us to take advantage of the self-veto effect in the southern sky reducing the atmospheric neutrino rate allowing us to detect astrophysical neutrinos to energies well below 100 TeV. We measure the astrophysical flux as $\phi_{\rm Astro}^{\rm per-flavor} = 1.68^{+0.19}_{-0.22} (at 100 TeV)$ and $\gamma_{\rm Astro} = 2.58^{+0.10}_{-0.09}$ assuming a single power law flux. The astrophysical flux 90% sensitive energy range is 3 TeV to 500 TeV, extending IceCube's reach to the low energy astrophysical flux by an order of magnitude. A brief summary of tests performed to search for neutrinos from the galactic plane using this dataset is also provided. With this sample, we did not find statistically significant evidence for emission from the galactic plane. We then tested the impact of these galactic plane neutrinos on the isotropic diffuse flux, with at most 10% effect on the overall normalization and negligible impact to the spectral index.

Corresponding authors: Manuel Silva¹, Sarah Mancina^{1,2}, Jesse Osborn^{1*}

- ¹ University of Wisconsin, Madison
- ² Università Degli Studi di Padova
- * Presenter

The 38th International Cosmic Ray Conference (ICRC2023) 26 July – 3 August, 2023 Nagoya, Japan



1. Introduction

High energy neutrinos of an astrophysical origin were discovered by IceCube in 2013 [1–3]. Since then, IceCube searches for sources of these neutrinos suggest a non-negligible flux in the direction of TXS 0506+056 [4, 5], NGC 1068 [6], and from Milky Way galactic plane emission [7, 8]. However, the flux seen from the sum of these sources is not sufficient to account for the total observed diffuse neutrino flux. Therefore, it is of great importance to measure the total astrophysical diffuse flux to infer properties of the production mechanisms of these neutrinos in a more model-independent manner. Historically, this is done assuming a single power law flux.

We first present a new data sample which relies on veto techniques and machine learning classification to reduce the muon rate in the southern sky while retaining a large sample of starting track events. These veto-based datasets also benefit from the self-veto effect [9–11] which is a suppression of the atmospheric neutrino rate in the southern sky due to the removal of atmospheric muons from the same shower. Starting track events occur when a muon neutrino undergoes a charged current deep inelastic scattering interaction within the fiducial volume of the detector. A large initial cascade is observed from the hadronic component of the interaction, which results in a neutrino energy resolution of $\sim 25-30\%$ between 1 TeV and 10 PeV. In addition, a muon track is produced in the interaction which is then used to reconstruct the neutrino direction. The resulting directional resolution is 1.6° at 1 TeV and improves to 0.66° at 100 TeV neutrino energies.

We then present a measurement of the astrophysical diffuse flux using 10.3 years of data. This measurement is first under the single power law flux assumption with a 90% sensitive energy range of 3 to 550 TeV. This is followed up with a more detailed measurement under the broken power law flux assumption. We also measure the flux as a sum of 8 single power law segments with a spectral index of $\gamma = 2$. We then present a search of astrophysical neutrino sources, in particular in the direction of the Milky Way galaxy under the *Fermi*-LAT π^0 [12] model assumption. Lastly, we estimate the contribution of these neutrinos from the galactic plane to the astrophysical diffuse flux.

2. Event Selection

The Enhanced Starting Track Event Selection (ESTES) [13–16] is a data sample within IceCube searching for starting track events. To reduce the overwhelming atmospheric muon background, the starting-track-veto (STV) was applied. The STV constructs a dynamic veto region using the properties of the muon track to determine how "starting-like" the individual event is. The probability of an event being an incoming muon is referred to as the p_{miss} and shown in Fig. 1. We note the atmospheric muons are reduced by about three orders magnitude with a small reduction in starting astrophysical neutrinos. The next significant cut is referred to as the "starting track BDT". We use the XGBoost classifier [17] to distinguish atmospheric muons against starting muon neutrino events. A cut is applied on the BDT score to further reduce the atmospheric muon rate to about a handful of expected muons per year. Further description of the BDT can found in references [13, 15]. A summary of the cuts applied in ESTES are shown in Fig. 2. We see a significant drop in the atmospheric muons while still retaining a significant number of neutrinos.

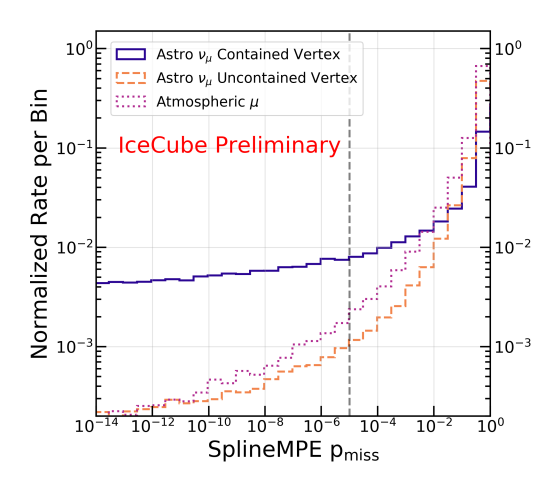


Figure 1: p_{miss} distribution for atmospheric muons and astrophysical neutrinos. A cut of $p_{miss} < 10^{-5}$ reduces atmospheric muon rates by three orders of magnitude. This figure is normalized to show p_{miss} shape differences between the interaction types.

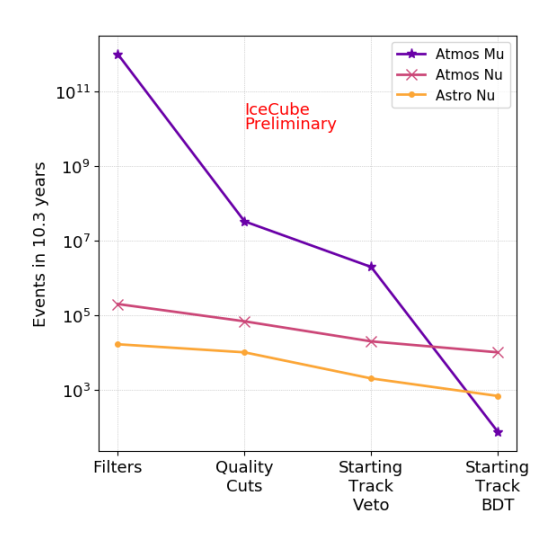


Figure 2: The atmospheric muon rate starts >5 orders of magnitude higher than the neutrino rate. After applying all the cuts, the neutrinos outnumber the muons by 2 orders of magnitude. The MC expectation shown is using benchmark models and shown for illustrative purposes only.

3. Astrophysical Diffuse Flux Measurement

A measurement of the astrophysical neutrino flux is performed using an isotropic single power law flux hypothesis (SPL) as shown in Eq. 1. This model assumes $\nu_e:\nu_\mu:\nu_\tau=1:1:1$ and $\nu:\bar{\nu}=1:1$ arriving at the surface of the Earth. In Eq. 1, $\phi_{\rm Astro}^{\rm per-flavor}$ refers to the per flavor normalization scaling factor and is defined as a unit-less number. We include a

$$\begin{split} & \Phi_{Astro}^{Total} = \phi_{Astro}^{per-flavor} \times (\frac{E_{\nu}}{100 \text{TeV}})^{-\gamma_{Astro}} \times C_{0}, \\ & C_{0} = 3 \times 10^{-18} \times \text{GeV}^{-1} \text{cm}^{-2} \text{s}^{-1} \text{sr}^{-1} \\ & \text{where,} \\ & \phi_{Astro}^{per-flavor} = 1.68^{+0.19}_{-0.22}, \quad \gamma_{Astro} = 2.58^{+0.10}_{-0.09} \end{split}$$

treatment of the conventional and prompt atmospheric neutrino flux and the atmospheric muons. This measurement is inclusive of detector systematics better described in an upcoming publication [16]. We measure a spectral index of $\gamma_{\rm Astro} = 2.58^{+0.10}_{-0.09}$ and per-flavor normalization of $\phi_{\rm Astro}^{\rm per flavor} = 1.68^{+0.19}_{-0.22}$ when measured at 100 TeV. The two-dimensional 68% confidence intervals (CI) for the two parameters of interest are shown in Fig. 4 using the profile likelihood assuming Wilks' theorem [18]. Within the 68% CI, all IceCube publications are consistent. Using the SPL, we then measure the 90% sensitive energy as 3-550 TeV making this measurement the lowest energy measurement to-date. We then measure the astrophysical diffuse flux as a sum of 8 segments (assuming a single power law with $\gamma = 2$) with results shown in Fig. 5 as black markers. All segments are consistent with a single power law.

Using the SPL flux measurement, we now show the best-fit Monte Carlo expectation and compare it to 10.3 years of data in Fig. 3. We observe excellent agreement with the data for all energy ranges and zenith angles of interest. In particular, the zenith distribution shows the

atmospheric muons rates greatly reduced with little reduction in the astrophysical neutrino rates. A tabular summary of the number of events is shown in Tab. 1 with and without a cut applied in the southern sky.

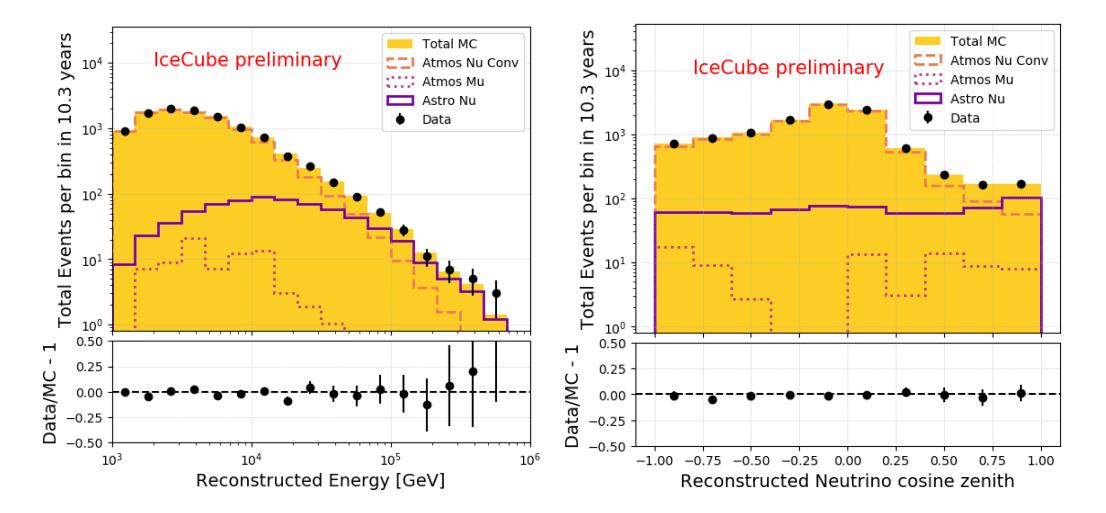


Figure 3: The reconstructed energy and cosine zenith distributions for data and Monte Carlo using the best-fit parameters from the single power law flux measurement. The astrophysical neutrinos are shown as a solid purple line, the atmospheric neutrino and muon expectations are shown as dashed and dotted lines respectively. (The prompt flux is not shown since the best-fit is 0.)

Given the sensitivity to sub-10 TeV energies, we then attempt to measure the astrophysical diffuse flux using a broken power law (BPL) shown analytically in Eq. 2. The BPL is modeled as two power laws at a distinct energy break; one spectral index for energies below and one above this break. This gives us a model-independent way to probe for structure in the neutrino flux towards lower energies. However, the BPL is found to be consistent with the SPL with a test-statistic of 0.4. As a result, E_{break}

$$\begin{split} & \Phi_{Astro}^{Total} = \phi_0 \times (\frac{E_{break}}{100 \text{TeV}})^{-\gamma_2} \times C_0, \\ & \phi_0 = \left\{ \begin{array}{l} \phi_{per-flavor}^{Astro} \times (\frac{E}{E_{break}})^{-\gamma_1} (E < E_{break}) \\ \phi_{per-flavor}^{Astro} \times (\frac{E}{E_{break}})^{-\gamma_2} (E > E_{break}) \end{array} \right. \\ & \text{where,} \\ & \phi_{per-flavor}^{Astro} = 1.7_{-0.22}^{+0.19}, \quad log_{10}(E_{break}) \sim 4.36 \\ & \gamma_1 = 2.79_{-0.50}^{+0.30}, \quad \gamma_2 = 2.52_{-0.09}^{+0.10} \end{split}$$

is poorly constrained, so we quote only the best fit point along with errors on γ_1 and γ_2 at that fixed E_{break} from one-dimensional profile likelihood scans. This result is shown in Fig. 5 as a gray line.

This result is in mild tension with the preference for a break around this energy with an index $\gamma_1 = 1.31^{+0.50}_{-1.21}$ presented in [19]. We note that the sensitivity of the ESTES sample to an astrophysical flux at these energies arises predominantly from the southern sky (declinations $\delta < -35^{\circ}$), while the analysis presented in [19] is sensitive over the entire sky. Non-isotropic contributions, such as from the Galactic plane [7] have not been considered in this broken power law hypothesis. In addition, systematic uncertainties have been parameterized differently in both analyses. Further investigations are ongoing about the potential impact of these parameterizations on the low-energy spectrum.

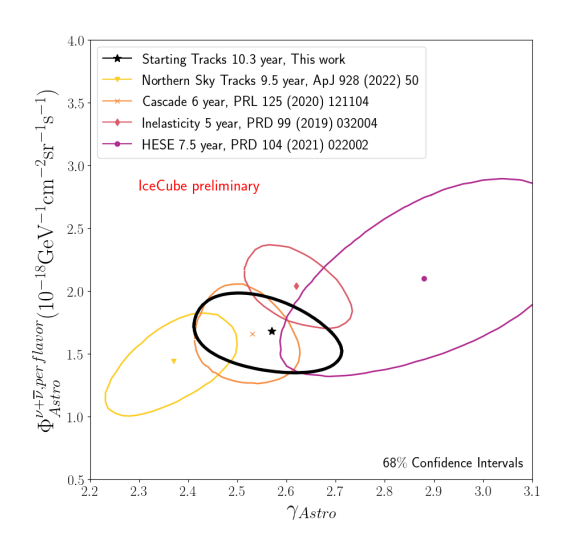


Figure 4: A summary of the SPL 68% confidence intervals for the Starting Tracks 10.3 year (this work) SPL measurement. We include recent IceCube results for direct comparison [20–23]. With these confidence intervals, all IceCube publications are consistent with this new result.

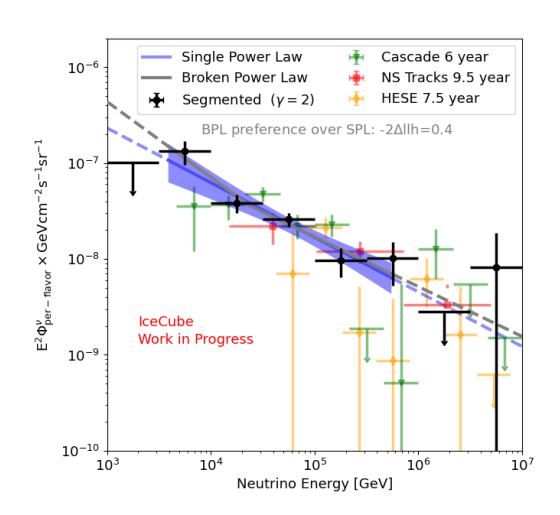


Figure 5: The blue line with error-band corresponds to the SPL measurement shown in Fig. 4. The shaded region is the 90% sensitive energy range computed using the SPL. The gray line is a fit to data assuming a broken power law flux. This model is not preferred in the data. The black points are the segmented power law flux measurement. We include results from recent IceCube publications for direct comparison [20, 21, 23].

	Events with Zenith < 80°	All Events
Astro Nu	298	680
Atmos Conv. Nu	980	10042
Atmos Conv. Mu	42	75
Total MC	1320	10797
Data	1365	10798

Table 1: A summary of observed data events and fitted MC events broken up by type under the single power law flux assumption. The left column has an additional cut on zenith $< 80^{\circ}$ to emphasize astrophysical neutrino purity in the southern sky.

4. Neutrino Sources from the Galactic Plane

The purity of ESTES in the southern sky made it of interest for searching for astrophysical neutrino sources. Four source hypotheses were tested including a search for neutrinos from the diffuse galactic plane (GP) emission. Under the diffuse galactic plane hypothesis, the same cosmic ray flux seen at earth is assumed to be propagating throughout our galaxy and produces neutrinos through pions generated when the cosmic rays interact with the galactic plane medium. Some of the most dense parts of the galactic plane, including the galactic center, are found in the southern sky where this event selection can improve upon previous IceCube searches with muon neutrinos due to the atmospheric neutrino self-veto effect.

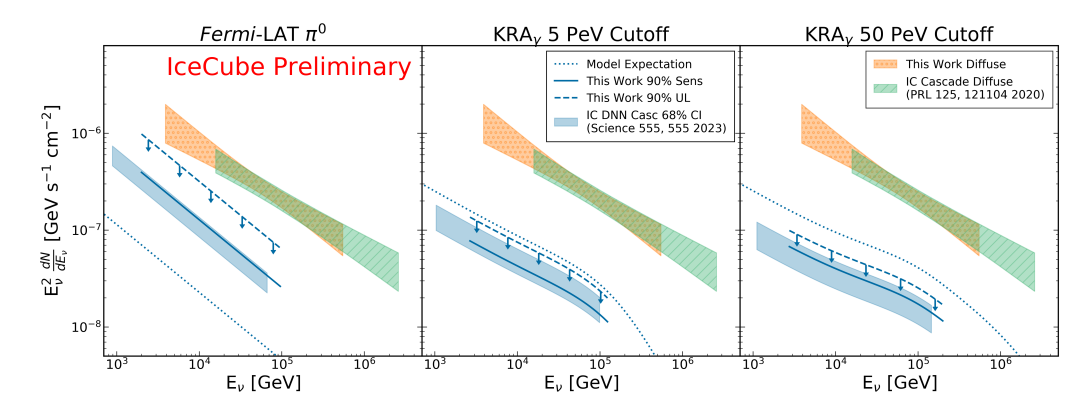


Figure 6: The 90% upper limits (blue dashed line) and 90% sensitivities (solid blue line) for ESTES on the GP template analyses compared to the DNN cascade 68% confidence interval (CI, blue shaded region) and the ESTES diffuse fit (orange shaded region) and Cascade diffuse fit (green shaded region). Each figure represents the diffuse galactic plane neutrino emission model tested: (Left) *Fermi-LAT* π^0 [12], (Center) KRA $_{\gamma}$ with a 5 PeV exponential energy cutoff, and (Right) KRA $_{\gamma}$ with a 50 PeV exponential energy cutoff [24] The energy range for this work's upper limit and sensitivity were calculated by injecting events according to the models spectral model and finding the central range where 90% of the expected events lie.

The results using only ESTES returned a post-trial p-value of 0.070 for the Fermi-LAT π^0 map [12], so we were unable to reject the null hypothesis. The search also looked for neutrinos correlated with the locations of three galactic plane source catalogs: supernova remnants, pulsar wind nebulae, and unidentified TeV galactic plane objects. The supernova remnants resulted in the largest test statistic and the post-trial p-value was found to be 0.056, meaning the null hypothesis could not be rejected. Figure 6 shows the 90% upper limits set by this analysis on the three galactic plane templates tested in comparison to the best fits produced by IceCube's DNN-based cascade event selection [7]. These upper limits are consistent with [7] and the sensitivity of this analysis.

We then use the GP flux from the DNNbased cascade sample [7] and include it as an additional parameter (with a Gaussian constraint) in the measurement of the diffuse flux from Sec. 3. Figure 7 shows the measurement performed without the galactic plane neutrinos (in black) and now included (in yellow) using the Fermi-LAT π^0 template. We observe a large shift in the astrophysical normalization of 10% with a negligible shift in the spectral index $(\Delta \gamma = 0.01)$. This observation is in agreement with an independent measurement of the diffuse flux using through-going tracks from the northern sky [25]. Therefore, it is recommended that future isotropic diffuse flux measurements include the galactic plane as was shown in this work.

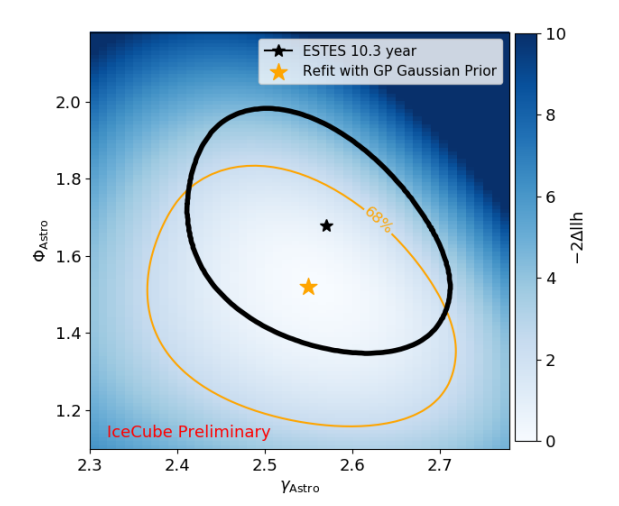


Figure 7: Single power law flux measurement as described in the primary text of this work (in black) and introducing the galactic plane as additional nuisance parameter in the fit (in yellow).

5. Conclusion

A new dataset using veto-techniques and boosted decision trees to search for starting track events in the northern and southern hemisphere was shown. We detected 10,798 events over the entire sky with 99.3% neutrino purity. This dataset found 1000 neutrinos of astrophysical origin with 1/3 of the astrophysical neutrinos localized to the southern sky.

This dataset was then used to measure the astrophysical neutrino flux using a single power law flux. The best-fit spectral index is $\gamma_{\rm Astro} = 2.58^{+0.10}_{-0.09}$ and per-flavor normalization is $\Phi_{\rm Astro}^{\rm per-flavor} = 1.68^{+0.19}_{-0.22}$ (at 100 TeV). The sensitive energy ranges for this particular flux model was defined as 3-550 TeV demonstrating the IceCube detector's ability to investigate the astrophysical neutrino flux with such precision in energy regions typically dominated by atmospheric backgrounds, below 16 TeV, for the first time. Assuming a single power law flux, we then presented a segmented measurement of the flux from 1 TeV to 10 PeV showing consistent segments with the single power law. Finally, a measurement of the flux under the broken power law assumption was performed. We tested a lower (higher) energy spectral index below (above) a break energy. We measured the BPL to be consistent with the SPL with a test-statistic of 0.4.

We observe consistency above 10 TeV for the SPL parameters with all other IceCube samples, including the latest, statistically independent, combined measurement [19]. Given that this analysis and [19] have different systematic uncertainties and use different event selections and reconstruction techniques, the flux below 10 TeV may be impacted by additional systematic effects, which require further study.

A time-integrated neutrino source search was preformed searching for galactic plane diffuse neutrino emission. No significant excesses are found; however, important limits are set on the hadronic emission from TeV gamma-ray galactic plane objects. The upper limits from the galactic plane template analysis are consistent with the recent results using IceCube cascade events to study diffuse neutrino emissions from cosmic ray interactions in the galactic plane. However, there are efforts within IceCube to combine starting tracks with the other data streams to fully comprehend the galactic plane neutrino emission using all of the morphological structures produced by neutrinos within IceCube [26].

Finally, we estimate the impact of the galactic plane neutrino emission under the Fermi π^0 flux model and concluded that while the expected impact on the diffuse flux spectral index is at the sub-percent level it can still contribute to the overall diffuse flux normalization by $\sim 10\%$.

References

- [1] IceCube Collaboration, M. G. Aartsen et al. Science 342 (2013) 1242856.
- [2] IceCube Collaboration, M. G. Aartsen et al. Phys. Rev. Lett. 111 (Jul, 2013) 021103.
- [3] IceCube Collaboration, M. G. Aartsen et al. Phys. Rev. Lett. 113 (2014) 101101.
- [4] **IceCube** Collaboration, M. G. Aartsen et al. Science **361** no. 6398, (2018) 147–151.
- [5] IceCube, Fermi-LAT, MAGIC, AGILE, ASAS-SN, HAWC, H.E.S.S., INTEGRAL, Kanata, Kiso, Kapteyn, Liverpool Telescope, Subaru, Swift NuSTAR, VERITAS, VLA/17B-403 Collaboration, M. G. Aartsen et al. Science 361 no. 6398, (2018) eaat1378.

- [6] **IceCube** Collaboration, R. Abbasi et al. Science 378 no. 6619, (2022) 538–543.
- [7] **IceCube** Collaboration, R. Abbasi et al. Science **555** no. 5555, (2023) 555–555.
- [8] **IceCube** Collaboration, S. Sclafani and M. Hünnefeld *PoS* **ICRC2023** (these proceedings) 1108.
- [9] S. Schönert, T. K. Gaisser, E. Resconi, and O. Schulz *Phys. Rev. D* **79** (Feb, 2009) 043009.
- [10] T. K. Gaisser, K. Jero, A. Karle, and J. van Santen Phys. Rev. D 90 (Jul, 2014) 023009.
- [11] C. A. Argüelles, S. Palomares-Ruiz, A. Schneider, L. Wille, and T. Yuan *Journal of Cosmology and Astroparticle Physics* **2018** no. 07, (Jul, 2018) 047–047.
- [12] **Fermi-LAT** Collaboration, M. Ackermann et al. Astrophys. J. **750** (2012) 3.
- [13] IceCube Collaboration, M. Silva and S. Mancina PoS ICRC2019 (2020) 1010.
- [14] IceCube Collaboration, S. Mancina and M. Silva PoS ICRC2019 (2020) 954.
- [15] IceCube Collaboration, R. Abbasi et al. PoS ICRC2021 (2021) 1130.
- [16] **IceCube** Collaboration, M. G. Aartsen et al. To be submitted to Physical Review D.
- [17] T. Chen and C. Guestrin, "XGBoost: A scalable tree boosting system," in *Proceedings of the 22nd ACM SIGKDD International Conference on Knowledge Discovery and Data Mining*, KDD '16, pp. 785–794. ACM, New York, NY, USA, 2016. http://doi.acm.org/10.1145/2939672.2939785.
- [18] S. S. Wilks The Annals of Mathematical Statistics 9 no. 1, (1938) 60 62.
- [19] **IceCube** Collaboration, R. Naab, E. Ganster, and Z. Zhang *PoS* **ICRC2023** (these proceedings) 1064.
- [20] IceCube Collaboration, R. Abbasi et al. Astrophys. J. 928 no. 1, (2022) 50.
- [21] IceCube Collaboration, M. G. Aartsen et al. Phys. Rev. Lett. 125 (Sep, 2020) 121104.
- [22] IceCube Collaboration, M. G. Aartsen et al. Phys. Rev. D 99 no. 3, (2019) 032004.
- [23] **IceCube** Collaboration, R. Abbasi et al. Phys. Rev. D **104** (Jul, 2021) 022002.
- [24] D. Gaggero, D. Grasso, A. Marinelli, A. Urbano, and M. Valli.
- [25] **IceCube** Collaboration, P. Fuerst *PoS* **ICRC2023** (these proceedings) 1046.
- [26] **IceCube** Collaboration, P. Savina, L. Lu, and T. Yuan *PoS* **ICRC2023** (these proceedings) 1010.

Full Author List: IceCube Collaboration

R. Abbasi¹⁷, M. Ackermann⁶³, J. Adams¹⁸, S. K. Agarwalla⁴⁰, ⁶⁴, J. A. Aguilar¹², M. Ahlers²², J.M. Alameddine²³, N. M. Amin⁴⁴, K. Andeen⁴², G. Anton²⁶, C. Argüelles¹⁴, Y. Ashida⁵³, S. Athanasiadou⁶³, S. N. Axani⁴⁴, X. Bai⁵⁰, A. Balagopal V.⁴⁰, M. Baricevic⁴⁰, S. W. Barwick³⁰, V. Basu⁴⁰, R. Bay⁸, J. J. Beatty²⁰, ²¹, J. Becker Tjus¹¹, ⁶⁵, J. Beise⁶¹, C. Bellenghi²⁷, C. Benning¹, S. BenZvi⁵², D. Berley¹⁹, E. Bernardini⁴⁸, D. Z. Besson³⁶, E. Blaufuss¹⁹, S. Blot⁶³, F. Bontempo³¹, J. Y. Book¹⁴, C. Boscolo Meneguolo⁴⁸, S. Böser⁴¹, O. Botner⁶¹, J. Böttcher¹, E. Bourbeau²², J. Braun⁴⁰, B. Brinson⁶, J. Brostean-Kaiser⁶³, R. T. Burley², R. S. Busse⁴³, D. Butterfield⁴⁰, M. A. Campana⁴⁹, K. Carloni¹⁴, E. G. Carnie-Bronca², S. Chattopadhyay^{40, 64}, N. Chau¹², C. Chen⁶, Z. Chen⁵⁵, D. Chirkin⁴⁰, S. Choi⁵⁶, B. A. Clark¹⁹, L. Classen⁴³, A. Coleman⁶¹, G. H. Collin¹⁵, A. Connolly²⁰, ²¹, J. M. Conrad¹⁵, P. Coppin¹³, P. Correa¹³, D. F. Cowen⁵⁹, ⁶⁰, P. Dave⁶, C. De Clercq¹³, J. J. DeLaunay⁵⁸, D. Delgado¹⁴, S. Deng¹, K. Deoskar⁵⁴, A. Desai⁴⁰, P. Desiati⁴⁰, K. D. de Vries¹³, G. de Wasseige³⁷, T. DeYoung²⁴, A. Diaz¹⁵, J. C. Díaz-Vélez⁴⁰, M. Dittmer⁴³, A. Domi²⁶, H. Dujmovic⁴⁰, M. A. DuVernois⁴⁰, T. Ehrhardt⁴¹, P. Eller²⁷, E. Ellinger⁶², S. El Mentawi¹, D. Elsässer²³, R. Engel^{31, 32}, H. Erpenbeck⁴⁰, J. Evans¹⁹, P. A. Evenson⁴⁴, K. L. Fan¹⁹, K. Fang⁴⁰, K. Farrag¹⁶, A. R. Fazely⁷, A. Fedynitch⁵⁷, N. Feigl¹⁰, S. Fiedlschuster²⁶, C. Finley⁵⁴, L. Fischer⁶³, D. Fox⁵⁹, A. Franckowiak¹¹, A. Fritz⁴¹, P. Fürst¹, J. Gallagher³⁹, E. Ganster¹, A. Garcia¹⁴, L. Gerhardt⁹, A. Ghadimi⁵⁸, C. Glaser⁶¹, T. Glauch²⁷, T. Glüsenkamp^{26, 61}, N. Goehlke³², J. G. Gonzalez⁴⁴, S. Goswami⁵⁸, D. Grant²⁴, S. J. Gray¹⁹, O. Gries¹, S. Griffin⁴⁰, S. Griswold⁵², K. M. Groth²², C. Günther¹, P. Gutjahr²³, C. Haack²⁶, A. Hallgren⁶¹, R. Halliday²⁴, L. Halve¹, F. Halzen⁴⁰, H. Hamdaoui⁵⁵, M. Ha Minh²⁷, K. Hanson⁴⁰, J. Hardin¹⁵, A. A. Harnisch²⁴, P. Hatch³³, A. Haungs³¹, K. Helbing⁶², J. Hellrung¹¹, F. Henningsen²⁷, L. Heuermann¹, N. Heyer⁶¹, S. Hickford⁶², A. Hidvegi⁵⁴, C. Hill¹⁶, G. C. Hill², K. D. Hoffman¹⁹, S. Hori⁴⁰, K. Hoshina⁴⁰, ⁶⁶, W. Hou³¹, T. Huber³¹, K. Hultqvist⁵⁴, M. Hünnefeld²³, R. Hussain⁴⁰, K. Hymon²³, S. In⁵⁶, A. Ishihara¹⁶, M. Jacquart⁴⁰, O. Janik¹, M. Jansson⁵⁴, G. S. Japaridze⁵, M. Jeong⁵⁶, M. Jin¹⁴, B. J. P. Jones⁴, D. Kang³¹, W. Kang⁵⁶, X. Kang⁴⁹, A. Kappes⁴³, D. Kappesser⁴¹, L. Kardum²³, T. Karg⁶³, M. Karl²⁷, A. Karle⁴⁰, U. Katz²⁶, M. Kauer⁴⁰, J. L. Kelley⁴⁰, A. Khatee Zathul⁴⁰, A. Kheirandish^{34, 35}, J. Kiryluk⁵⁵, S. R. Klein^{8, 9}, A. Kochocki²⁴, R. Koirala⁴⁴, H. Kolanoski¹⁰, T. Kontrimas²⁷, L. Köpke⁴¹, C. Kopper²⁶, D. J. Koskinen²², P. Koundal³¹, M. Kovacevich⁴⁹, M. Kowalski^{10, 63}, T. Kozynets²², J. Krishnamoorthi^{40, 64}, K. Kruiswijk³⁷, E. Krupczak²⁴, A. Kumar⁶³, E. Kun¹¹, N. Kurahashi⁴⁹, N. Lad⁶³, C. Lagunas Gualda⁶³, M. Lamoureux³⁷, M. J. Larson¹⁹, S. Latseva¹, F. Lauber⁶², J. P. Lazar^{14, 40}, J. W. Lee⁵⁶, K. Leonard DeHolton⁶⁰, A. Leszczyńska⁴⁴, M. Lincetto¹¹, Q. R. Liu⁴⁰, M. Liubarska²⁵, E. Lohfink⁴¹, C. Love⁴⁹, C. J. Lozano Mariscal⁴³, L. Lu⁴⁰, F. Lucarelli²⁸, W. Luszczak^{20, 21}, Y. Lyu^{8, 9}, J. Madsen⁴⁰, K. B. M. Mahn²⁴, Y. Makino⁴⁰, E. Manao²⁷, S. Mancina^{40, 48}, W. Marie Sainte⁴⁰, I. C. Mariş¹², S. Marka⁴⁶, Z. Marka⁴⁶, M. Marsee⁵⁸, I. Martinez-Soler¹⁴, R. Maruyama⁴⁵, F. Mayhew²⁴, T. McElroy²⁵, F. McNally³⁸, J. V. Mead²², K. Meagher⁴⁰, S. Mechbal⁶³, A. Medina²¹, M. Meier¹⁶, Y. Merckx¹³, L. Merten¹¹, J. Micallef²⁴, J. Mitchell⁷, T. Montaruli²⁸, R. W. Moore²⁵, Y. Morii¹⁶, R. Morse⁴⁰, M. Moulai⁴⁰, T. Mukherjee³¹, R. Naab⁶³, R. Nagai¹⁶, M. Nakos⁴⁰, U. Naumann⁶², J. Necker⁶³, A. Negi⁴, M. Neumann⁴³, H. Niederhausen²⁴, M. U. Nisa²⁴, A. Noell¹, A. Novikov⁴⁴, S. C. Nowicki²⁴, A. Obertacke Pollmann¹⁶, V. O'Dell⁴⁰, M. Oehler³¹, B. Oeyen²⁹, A. Olivas¹⁹, R. Ørsøe²⁷, J. Osborn⁴⁰, E. O'Sullivan⁶¹, H. Pandya⁴⁴, N. Park³³, G. K. Parker⁴, E. N. Paudel⁴⁴, L. Paul^{42, 50}, C. Pérez de los Heros⁶¹, J. Peterson⁴⁰, S. Philippen¹, A. Pizzuto⁴⁰, M. Plum⁵⁰, A. Pontén⁶¹, Y. Popovych⁴¹, M. Prado Rodriguez⁴⁰, B. Pries²⁴, R. Procter-Murphy¹⁹, G. T. Przybylski⁹, C. Raab³⁷, J. Rack-Helleis⁴¹, K. Rawlins³, Z. Rechav⁴⁰, A. Rehman⁴⁴, P. Reichherzer¹¹, G. Renzi¹², E. Resconi²⁷, S. Reusch⁶³, W. Rhode²³, B. Riedel⁴⁰, A. Rifaie¹, E. J. Roberts², S. Robertson⁸, 9, S. Rodan⁵⁶, G. Roellinghoff⁵⁶, M. Rongen²⁶, C. Rott⁵³, 56, T. Ruhe²³, L. Ruohan²⁷, D. Ryckbosch²⁹, I. Safa¹⁴, ⁴⁰, J. Saffer³², D. Salazar-Gallegos²⁴, P. Sampathkumar³¹, S. E. Sanchez Herrera²⁴, A. Sandrock⁶², M. Santander⁵⁸, S. Sarkar²⁵, S. Sarkar⁴⁷, J. Savelberg¹, P. Savina⁴⁰, M. Schaufel¹, H. Schieler³¹, S. Schindler²⁶, L. Schlickmann¹, B. Schlüter⁴³, F. Schlüter¹², N. Schmeisser⁶², T. Schmidt¹⁹, J. Schneider²⁶, F. G. Schröder³¹, ⁴⁴, L. Schumacher²⁶, G. Schwefer¹, S. Sclafani¹⁹, D. Seckel⁴⁴, M. Seikh³⁶, S. Seunarine⁵¹, R. Shah⁴⁹, A. Sharma⁶¹, S. Shefali³², N. Shimizu¹⁶, M. Silva⁴⁰, B. Skrzypek¹⁴, B. Smithers⁴, R. Snihur⁴⁰, J. Soedingrekso²³, A. Søgaard²², D. Soldin³², P. Soldin¹, G. Sommani¹¹, C. Spannfellner²⁷, G. M. Spiczak⁵¹, C. Spiering⁶³, M. Stamatikos²¹, T. Stanev⁴⁴, T. Stezelberger⁹, T. Stürwald⁶², T. Stuttard²², G. W. Sullivan¹⁹, I. Taboada⁶, S. Ter-Antonyan⁷, M. Thiesmeyer¹, W. G. Thompson¹⁴, J. Thwaites⁴⁰, S. Tilav⁴⁴, K. Tollefson²⁴, C. Tönnis⁵⁶, S. Toscano¹², D. Tosi⁴⁰, A. Trettin⁶³, C. F. Tung⁶, R. Turcotte³¹, J. P. Twagirayezu²⁴, B. Ty⁴⁰, M. A. Unland Elorrieta⁴³, A. K. Upadhyay^{40, 64}, K. Upshaw⁷, N. Valtonen-Mattila⁶¹, J. Vandenbroucke⁴⁰, N. van Eijndhoven¹³, D. Vannerom¹⁵, J. van Santen⁶³, J. Vara⁴³, J. Veitch-Michaelis⁴⁰, M. Venugopal³¹, M. Vereecken³⁷, S. Verpoest⁴⁴, D. Veske⁴⁶, A. Vijai¹⁹, C. Walck⁵⁴, C. Weaver²⁴, P. Weigel¹⁵, A. Weindl³¹, J. Weldert⁶⁰, C. Wendt⁴⁰, J. Werthebach²³, M. Weyrauch³¹, N. Whitehorn²⁴, C. H. Wiebusch¹, N. Willey²⁴, D. R. Williams⁵⁸, L. Witthaus²³, A. Wolf¹, M. Wolf²⁷, G. Wrede²⁶, X. W. Xu⁷, J. P. Yanez²⁵, E. Yildizci⁴⁰, S. Yoshida¹⁶, R. Young³⁶, F. Yul⁴, S. Yu²⁴, T. Yuan⁴⁰, Z. Zhang⁵⁵, P. Zhelnin¹⁴, M. Zimmerman⁴⁰

¹ III. Physikalisches Institut, RWTH Aachen University, D-52056 Aachen, Germany

² Department of Physics, University of Adelaide, Adelaide, 5005, Australia

³ Dept. of Physics and Astronomy, University of Alaska Anchorage, 3211 Providence Dr., Anchorage, AK 99508, USA

⁴ Dept. of Physics, University of Texas at Arlington, 502 Yates St., Science Hall Rm 108, Box 19059, Arlington, TX 76019, USA

⁵ CTSPS, Clark-Atlanta University, Atlanta, GA 30314, USA

⁶ School of Physics and Center for Relativistic Astrophysics, Georgia Institute of Technology, Atlanta, GA 30332, USA

⁷ Dept. of Physics, Southern University, Baton Rouge, LA 70813, USA

⁸ Dept. of Physics, University of California, Berkeley, CA 94720, USA

⁹ Lawrence Berkeley National Laboratory, Berkeley, CA 94720, USA

 $^{^{\}rm 10}$ Institut für Physik, Humboldt-Universität zu Berlin, D-12489 Berlin, Germany

¹¹ Fakultät für Physik & Astronomie, Ruhr-Universität Bochum, D-44780 Bochum, Germany

¹² Université Libre de Bruxelles, Science Faculty CP230, B-1050 Brussels, Belgium

- ¹³ Vrije Universiteit Brussel (VUB), Dienst ELEM, B-1050 Brussels, Belgium
- ¹⁴ Department of Physics and Laboratory for Particle Physics and Cosmology, Harvard University, Cambridge, MA 02138, USA
- ¹⁵ Dept. of Physics, Massachusetts Institute of Technology, Cambridge, MA 02139, USA
- ¹⁶ Dept. of Physics and The International Center for Hadron Astrophysics, Chiba University, Chiba 263-8522, Japan
- ¹⁷ Department of Physics, Loyola University Chicago, Chicago, IL 60660, USA
- ¹⁸ Dept. of Physics and Astronomy, University of Canterbury, Private Bag 4800, Christchurch, New Zealand
- ¹⁹ Dept. of Physics, University of Maryland, College Park, MD 20742, USA
- ²⁰ Dept. of Astronomy, Ohio State University, Columbus, OH 43210, USA
- ²¹ Dept. of Physics and Center for Cosmology and Astro-Particle Physics, Ohio State University, Columbus, OH 43210, USA
- ²² Niels Bohr Institute, University of Copenhagen, DK-2100 Copenhagen, Denmark
- ²³ Dept. of Physics, TU Dortmund University, D-44221 Dortmund, Germany
- ²⁴ Dept. of Physics and Astronomy, Michigan State University, East Lansing, MI 48824, USA
- ²⁵ Dept. of Physics, University of Alberta, Edmonton, Alberta, Canada T6G 2E1
- ²⁶ Erlangen Centre for Astroparticle Physics, Friedrich-Alexander-Universität Erlangen-Nürnberg, D-91058 Erlangen, Germany
- ²⁷ Technical University of Munich, TUM School of Natural Sciences, Department of Physics, D-85748 Garching bei München, Germany
- ²⁸ Département de physique nucléaire et corpusculaire, Université de Genève, CH-1211 Genève, Switzerland
- ²⁹ Dept. of Physics and Astronomy, University of Gent, B-9000 Gent, Belgium
- ³⁰ Dept. of Physics and Astronomy, University of California, Irvine, CA 92697, USA
- ³¹ Karlsruhe Institute of Technology, Institute for Astroparticle Physics, D-76021 Karlsruhe, Germany
- ³² Karlsruhe Institute of Technology, Institute of Experimental Particle Physics, D-76021 Karlsruhe, Germany
- ³³ Dept. of Physics, Engineering Physics, and Astronomy, Queen's University, Kingston, ON K7L 3N6, Canada
- ³⁴ Department of Physics & Astronomy, University of Nevada, Las Vegas, NV, 89154, USA
- ³⁵ Nevada Center for Astrophysics, University of Nevada, Las Vegas, NV 89154, USA
- ³⁶ Dept. of Physics and Astronomy, University of Kansas, Lawrence, KS 66045, USA
- ³⁷ Centre for Cosmology, Particle Physics and Phenomenology CP3, Université catholique de Louvain, Louvain-la-Neuve, Belgium
- ³⁸ Department of Physics, Mercer University, Macon, GA 31207-0001, USA
- ³⁹ Dept. of Astronomy, University of Wisconsin-Madison, Madison, WI 53706, USA
- ⁴⁰ Dept. of Physics and Wisconsin IceCube Particle Astrophysics Center, University of Wisconsin–Madison, Madison, WI 53706, USA
- ⁴¹ Institute of Physics, University of Mainz, Staudinger Weg 7, D-55099 Mainz, Germany
- ⁴² Department of Physics, Marquette University, Milwaukee, WI, 53201, USA
- ⁴³ Institut für Kernphysik, Westfälische Wilhelms-Universität Münster, D-48149 Münster, Germany
- ⁴⁴ Bartol Research Institute and Dept. of Physics and Astronomy, University of Delaware, Newark, DE 19716, USA
- ⁴⁵ Dept. of Physics, Yale University, New Haven, CT 06520, USA
- ⁴⁶ Columbia Astrophysics and Nevis Laboratories, Columbia University, New York, NY 10027, USA
- ⁴⁷ Dept. of Physics, University of Oxford, Parks Road, Oxford OX1 3PU, United Kingdom
- ⁴⁸ Dipartimento di Fisica e Astronomia Galileo Galilei, Università Degli Studi di Padova, 35122 Padova PD, Italy
- ⁴⁹ Dept. of Physics, Drexel University, 3141 Chestnut Street, Philadelphia, PA 19104, USA
- ⁵⁰ Physics Department, South Dakota School of Mines and Technology, Rapid City, SD 57701, USA
- ⁵¹ Dept. of Physics, University of Wisconsin, River Falls, WI 54022, USA
- ⁵² Dept. of Physics and Astronomy, University of Rochester, Rochester, NY 14627, USA
- ⁵³ Department of Physics and Astronomy, University of Utah, Salt Lake City, UT 84112, USA
- ⁵⁴ Oskar Klein Centre and Dept. of Physics, Stockholm University, SE-10691 Stockholm, Sweden
- ⁵⁵ Dept. of Physics and Astronomy, Stony Brook University, Stony Brook, NY 11794-3800, USA
- ⁵⁶ Dept. of Physics, Sungkyunkwan University, Suwon 16419, Korea
- ⁵⁷ Institute of Physics, Academia Sinica, Taipei, 11529, Taiwan
- ⁵⁸ Dept. of Physics and Astronomy, University of Alabama, Tuscaloosa, AL 35487, USA
- ⁵⁹ Dept. of Astronomy and Astrophysics, Pennsylvania State University, University Park, PA 16802, USA
- 60 Dept. of Physics, Pennsylvania State University, University Park, PA 16802, USA
- ⁶¹ Dept. of Physics and Astronomy, Uppsala University, Box 516, S-75120 Uppsala, Sweden
- 62 Dept. of Physics, University of Wuppertal, D-42119 Wuppertal, Germany
- ⁶³ Deutsches Elektronen-Synchrotron DESY, Platanenallee 6, 15738 Zeuthen, Germany
- ⁶⁴ Institute of Physics, Sachivalaya Marg, Sainik School Post, Bhubaneswar 751005, India
- ⁶⁵ Department of Space, Earth and Environment, Chalmers University of Technology, 412 96 Gothenburg, Sweden
- ⁶⁶ Earthquake Research Institute, University of Tokyo, Bunkyo, Tokyo 113-0032, Japan

Acknowledgements

The authors gratefully acknowledge the support from the following agencies and institutions: USA – U.S. National Science Foundation-Office of Polar Programs, U.S. National Science Foundation-Physics Division, U.S. National Science Foundation-EPSCoR, Wisconsin Alumni Research Foundation, Center for High Throughput Computing (CHTC) at the University of Wisconsin–Madison, Open Science

Grid (OSG), Advanced Cyberinfrastructure Coordination Ecosystem: Services & Support (ACCESS), Frontera computing project at the Texas Advanced Computing Center, U.S. Department of Energy-National Energy Research Scientific Computing Center, Particle astrophysics research computing center at the University of Maryland, Institute for Cyber-Enabled Research at Michigan State University, and Astroparticle physics computational facility at Marquette University; Belgium – Funds for Scientific Research (FRS-FNRS and FWO), FWO Odysseus and Big Science programmes, and Belgian Federal Science Policy Office (Belspo); Germany – Bundesministerium für Bildung und Forschung (BMBF), Deutsche Forschungsgemeinschaft (DFG), Helmholtz Alliance for Astroparticle Physics (HAP), Initiative and Networking Fund of the Helmholtz Association, Deutsches Elektronen Synchrotron (DESY), and High Performance Computing cluster of the RWTH Aachen; Sweden – Swedish Research Council, Swedish Polar Research Secretariat, Swedish National Infrastructure for Computing (SNIC), and Knut and Alice Wallenberg Foundation; European Union – EGI Advanced Computing for research; Australia – Australian Research Council; Canada – Natural Sciences and Engineering Research Council of Canada, Calcul Québec, Compute Ontario, Canada Foundation for Innovation, WestGrid, and Compute Canada; Denmark – Villum Fonden, Carlsberg Foundation, and European Commission; New Zealand – Marsden Fund; Japan – Japan Society for Promotion of Science (JSPS) and Institute for Global Prominent Research (IGPR) of Chiba University; Korea – National Research Foundation of Korea (NRF); Switzerland – Swiss National Science Foundation (SNSF); United Kingdom – Department of Physics, University of Oxford.